Electronic Supplementary Material (ESI) for New Journal of Chemistry.
This journal is © The Royal Society of Chemistry and the Centre National de la Recherche Scientifique 2023

Copper-guided tuning of supramolecular nano-assembly in pseudopeptide-based soft bioinspired materials

*Arpna Tamrakar, Kamlesh Kumar Nigam and Mrituanjay D. Pandey**

Department of Chemistry, Institute of Science, Banaras Hindu University, Varanasi- 221005 UP, India. Email: mdpandey.chem@bhu.ac.in

Content: -

1. **Fig. S1: -** ^{1}H NMR spectra of **1** in $CDCl_3$
2. **Fig. S2: -** ^{13}C NMR spectra of **1** in $CDCl_3$.
3. **Fig. S3: -** HRMS (ESI-TOF) spectra of **1.**
4. **Fig. S4: -** ^{1}H NMR spectra of **2** in $CDCl_3$.
5. **Fig. S5: -** ^{13}C NMR spectra of **2** in $CDCl_3$.
6. **Fig. S6: -** HRMS (ESI-TOF) spectra of **2**.
7. **Fig. S7: -** UV-Visible spectra of **1** and **2** in EtOH: Water (7:3, v/v, at r.t.).
8. **Fig. S8: -** UV-Visible titration of the stock solution of **1** and **2** with the conjugative addition of Cu(II) ions (0-10 equiv.) in EtOH: Water (7:3, v/v, at r.t.).
9. **Fig. S9: -** Fluorescence spectra of **1** and **2** (10μM) in EtOH: Water (7:3, v/v, at r.t.).
10. **Fig. S10: -** Fluorescence sensing of **1** and **2** (10μM) with various anion in EtOH: Water (7:3, v/v, at r.t.).
11. **Table S1**: - Quantum yield of 1 and 2 with and without the addition of Cu(II) ions.

12. **Fig. S11:-** Lifetime spectra of stock solution of **1** (a) and **2** (b) (neat) and with the addition of Cu(II) ions in EtOH: Water (7:3, v/v at r.t.) solution
13. **Table S2** Fluorescence decay parameters of pseudopeptidic probes **1** and **2** in ethanol-water solution (4:6, v/v, at rt.).
14. **Fig. S12 -** Stern-Volmer plot of **1** (a) and **2** (b) with respect to the concentration of Cu(II) ions in EtOH: Water (7:3, v/v, at r.t.).
15. **Fig. S13: -** Jobs plot of aqueous stock solution of **1** (a) and **2** (b) toward varying concentrations of Cu(II) ions in ETOH: Water (7:3, v/v, at r.t.)
16. **Fig. S14:-** Interference experiments of aqueous stock solution of **1** (a) and **2** (b) toward Cu(II) ions and other metal ions in EtOH: Water (7:3, v/v, at r.t.)
17. **Fig. S15: -** Interference experiments of aqueous stock solution of **1** (a) and **2** (b) toward Cu(II) ions and other anions in EtOH: Water (7:3, v/v, at r.t.).
18. **Fig. S16:** - Benesi-Hildebrand plot of **1** (a) and **2** (B) with the varying concentration of Cu(II) ions in EtOH: Water (7:3, v/v, rt.)
19. **Fig. S17:** - Fluorescence sensitivity of **1** (a) and **2** (b) in the presence of a different concentration of Cu(II) (10^{-11} to 10^{-3} M) ions in EtOH: Water (7:3, v/v, at r.t.)
20. **Fig. S18: - (a)** Fluorescence sensitivity of **1** in the presence of a different concentration of Cu(II) (1 x 10^{-7} to 9 x 10^{-7} M) ions in EtOH: Water (7:3, v/v, at r.t.). (b) Fluorescence sensitivity of **2** in the presence of a different concentration of Cu(II) (1 x 10^{-8} to 9 x 10^{-8} M) ions in EtOH:Water (7:3, v/v, at r.t.).
21. **Fig. S19:** - CD spectra of stock solution of chemosensor **1** (A) and **2** (B) (neat) and with the addition of Cu(II) ions in pure ethanol solution.
22. **Table S3:-** Comparison with previously reported fluorescence-based sensors for Cu(II) ions.

23. **Fig. S20:** - Reversibility plot of 1 and 2 with respect to the addition of Cu(II) ion and EDTA solution.
24. **Fig. S21:** - HRMS (ESI-TOF) spectra of **1**+Cu(II).
25. **Fig. S22:** -HRMS (ESI-TOF) spectra of **2**+Cu(II).
26. **Fig. S23:** - The FT-IR deconvolution spectrum of **1**+Cu(II) and **2**+Cu(II).
27. **Fig. S24:** - Electron microscopy images of self-assembly neat **1** (a) 2D representation. (b) zoomed image of the 2D representation of **1**. (c) Average particle size distribution of **1**. (d) 2D representation of self-assembly of **1**+Cu(II). (e) Zoomed image of the 2D representation of **1**+Cu(II). (f) Average particle size distribution of **1**+Cu(II).
28. **Fig. S25:** - Electron microscopy images of self-assembly neat **2**, (a) 2D representation. (b) zoomed image of the 2D representation of **2**. (c) Average particle size distribution of **2**. (d) 2D representation of **2**+Cu(II). (e) Zoomed image of 2D representation of **2**+Cu(II). (f) Average particle size distribution of **2**+Cu(II).
29. **Table S4:** - Quantitative determination of spiked quantity of Cu(II) ions in the various water sample.
30. **Fig. S26**: - Lifetime spectra of stock solution of **1** (a) and **2** (b) (neat) and with the addition of various concentrations of Cu(II) ions (0-10equiv.) in EtOH:Water (7:3, v/v at r.t.) solution.
31. **Table S5:** - Fluorescence decay parameters of pseudopeptidic probes **1** and **2** on addition of various concentrations of Cu(II) ions (0-10equiv.) in ethanol-water solution (7:3, v/v, at rt.).

Experimental details: -

Materials and Methods: -

UV- visible spectra were recorded on an Agilent Cary 60 single beam, UV-Visible spectrometer with serial no. - MY19329220, and fluorescence spectra were measured on a Fluoromax 4CP plus spectrofluorometer with a 10 mm quartz cell at 25^{o}C. while fluorescence lifetime measurement was recorded on WITEC alpha300 Focus innovation, using pulse diode laser. ^{1}H and ^{13}C-NMR spectra were recorded on a JEOL AL 300 FT-NMR at an operating frequency of 500 MHz (^{1}H) and 126 MHz (^{13}C), respectively. Spectrometer operation at 500 MHz and 126 MHz in $CDCl_3$ solutions respectively are given in parts per million (ppm) related to Tetramethyl silane (TMS, δ = 0.00ppm). High-resolution mass spectra (ESI-HRMS) were recorded on SCIEX X500R (TOF-MS) mass spectrometer. FTIR spectra of all compounds are performed in solid state (using KBr pellet) in the 500-4000 cm^{-1} range. Melting point was measured using a Navyug (India) ISO-9001-2008 melting point apparatus. In the AFM study neat solution of 1 (10 μM) and 2 (10 μM) in ethanol:water and solution of 1 and 2 with the addition of Cu(II)ion (10 mM) by maintaining the total concentration of solution 10 μM was drop cast on a coverslip and dried in dust free environment using vacuum desicators. The samples were placed on a microscope (NT-MDT, Model: Solvernext) operating under semi-contact or tapping mode with the aid of a cantilever (NSG 01, silicone probe) with a resonating frequency was 230 kHz. the image was taken at room temperature with a scan speed of 0.5Hz, the data analysis was done using Nova px software. CD spectra were recorded on CD Polarimeter J-1500 made by JASKO at room temperature where the spectra were recorded of 10μM of neat **1** and **2** and with the addition of Cu(II) ion in pure ethanol solvent.

All chemicals are purchased from a commercial supplier and used without further purification. Lithium hydroxide and L-valine, L-phenylalanine were purchased from spectrochem. 4-(diethylamino) salicylaldehyde was purchased from TCI, and sodium borohydride was purchased from S. d. fine. Metal salts $Ni(NO_3)_2{\cdot}6H_2O$, $AgNO_3$, $Pb(NO_3)_2$, $Cd(NO_3)_2{\cdot}4H_2O$, KNO_3, $Co(NO_3)_2{\cdot}6H_2O$, $Hg(NO_3)_2$, $Ca(NO_3)_2{\cdot}4H_2O$, $Cu(NO_3)_2{\cdot}3H_2O$, $NaNO_3$, $Zn(NO_3)_2$, were purchased from Himedia.

The benesi-Hildebrand equation is used to calculate the value of the association constant.

$$1/I\text{-}I_0 = 1/ K_a [Cu(II)]^2 [I_{max} – I_0] + 1/ I_{max} \text{-}I_0$$

I_0 is the emission intensity of **1** and **2** when excited at 435 nm and 476 nm respectively, I is the emission intensity of the **1**+Cu(II) and **2**+Cu(II) (varying with the concentration of Cu(II)), I_{max} is the intensity of **1**+Cu(II) and **2**+Cu(II) complex respectively at the maximum concentration of analyte (Cu(II)), K_a is association constant. The value of the association constant (Ka) was calculated by the plot $1/I\text{-}I_0$ Vs 1/[Cu(II)].

The classical Stern-Volmer equation explores the quenching of **1** and **2** on the addition of Cu(II) ions.

$$I_0/I = 1 + K_{sv} [Q]$$

Where I_0 is the emission intensity of the solution of **1** and **2** (10μM). I is the emission intensity of **1** and **2** (10μM) with Cu(II) ions (10mM), respectively. [Q] represents the Cu(II) ions concentration, and K_{sv} represents, the Stern-Volmer quenching constant for **1** and **2** respectively.

Water samples preparation for Cu(II) detection: - To analyze the copper content in different water samples, Pond water (PW), River water (RW), distilled water (DW), and Tap water (TW),

were collected. All water samples were pretreated by boiling and filtration to avoid insoluble impurities, before being used for the detection of copper content analysis by **1** and **2.** To remove dissolved salts like chlorine content from water samples, they were boiled for one hour and then cooled at room temperature.

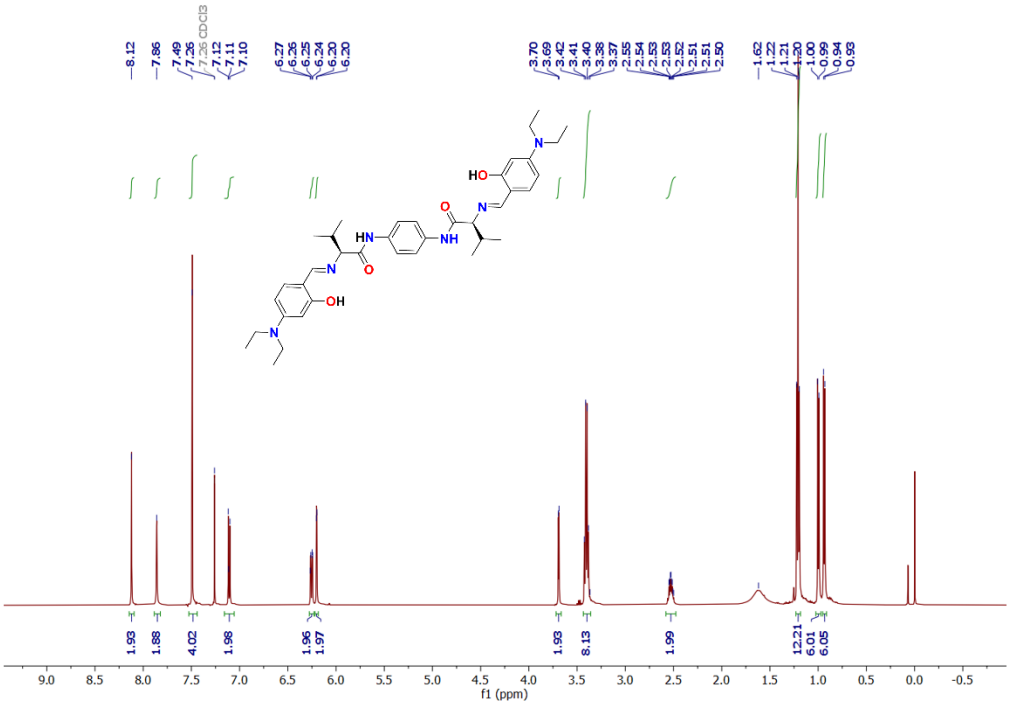

Fig. S1: - ^{1}H NMR spectra of **1** in $CDCl_3$.

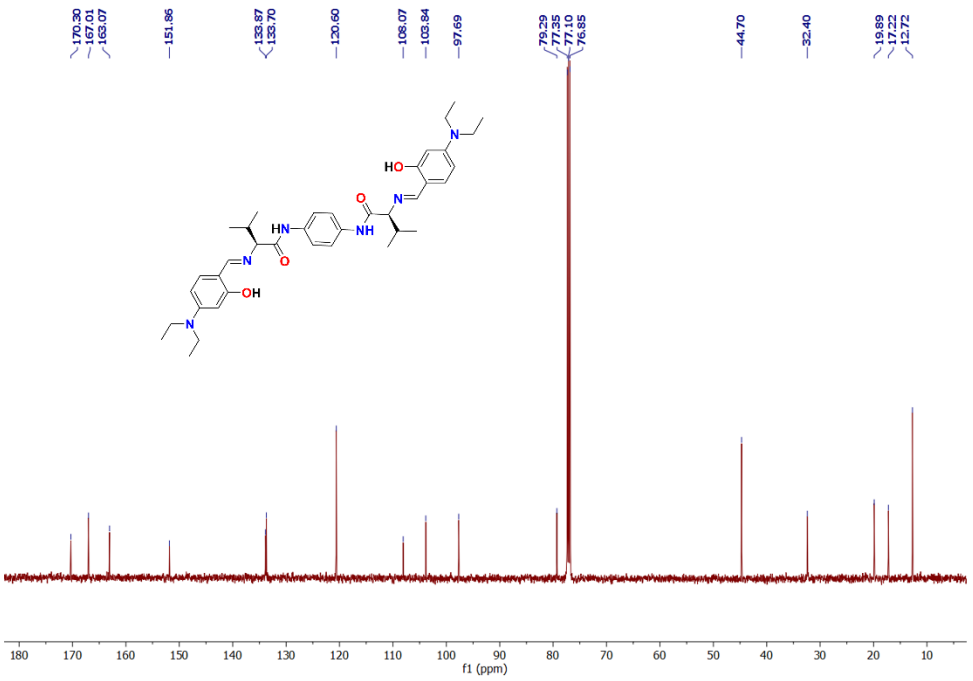

Fig. S2: - ^{13}C NMR spectra of **1** in $CDCl_3$.

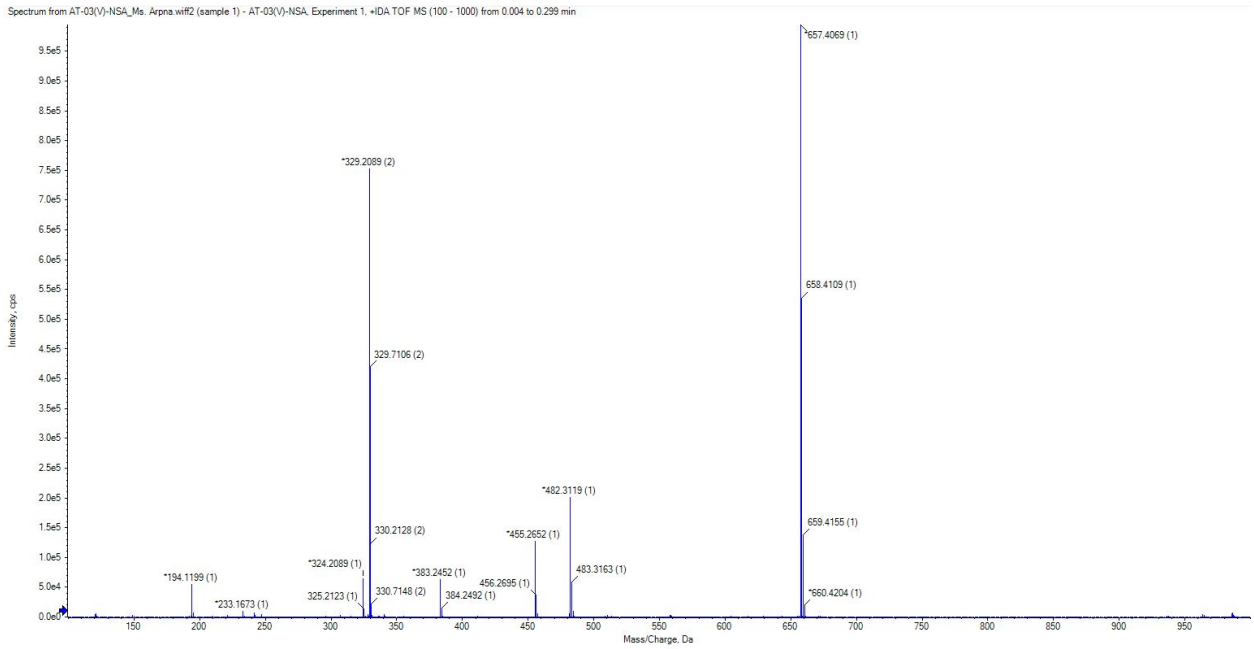

Fig. S3: - HRMS (ESI-TOF) spectra of **1.**

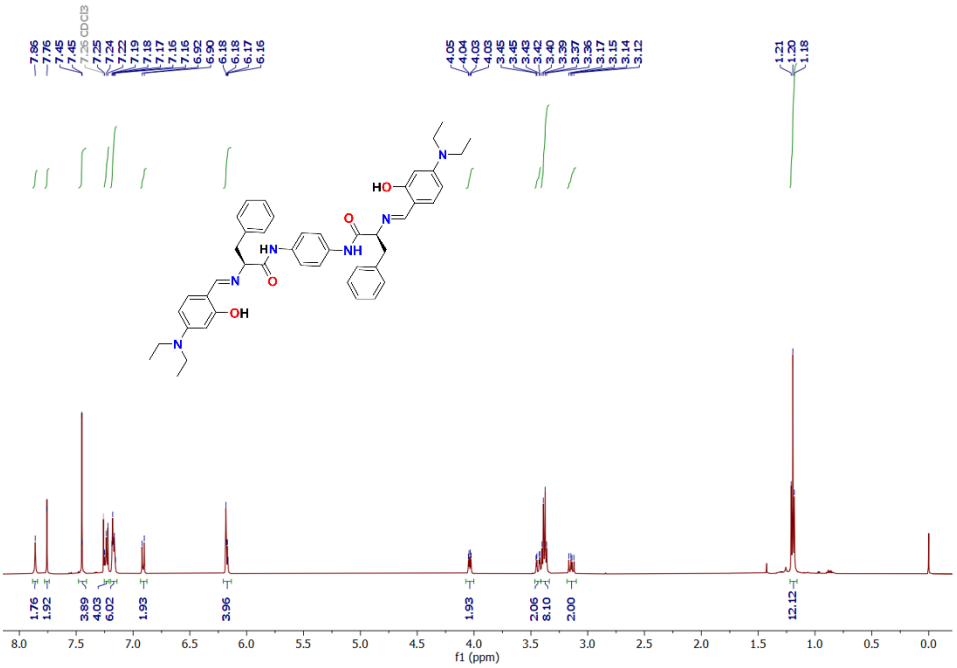

Fig. S4: - ^{1}H NMR spectra of **2** in $CDCl_3$.

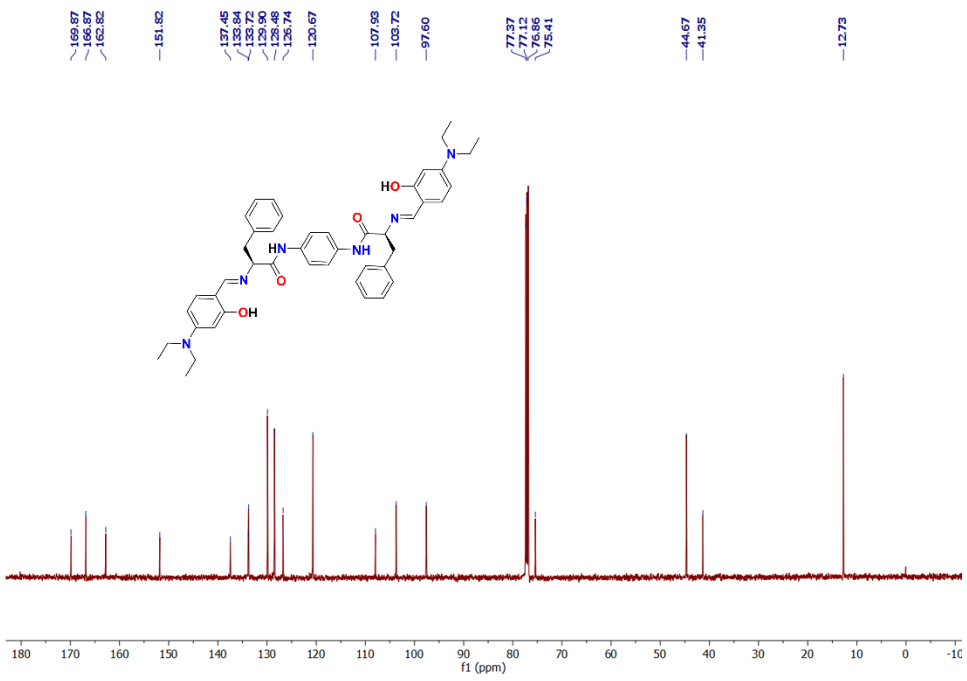

Fig. S5: - ^{13}C NMR spectra of **2** in $CDCl_3$.

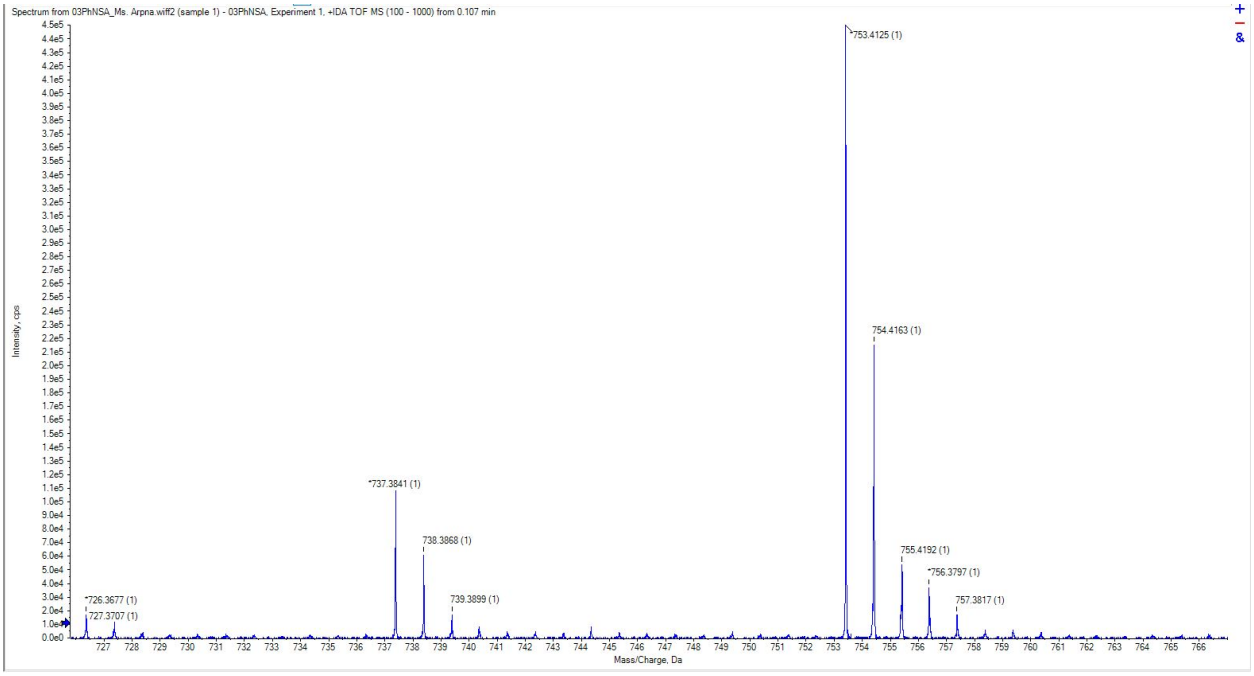

Fig. S6: - HRMS (ESI-TOF) spectra of **2**.

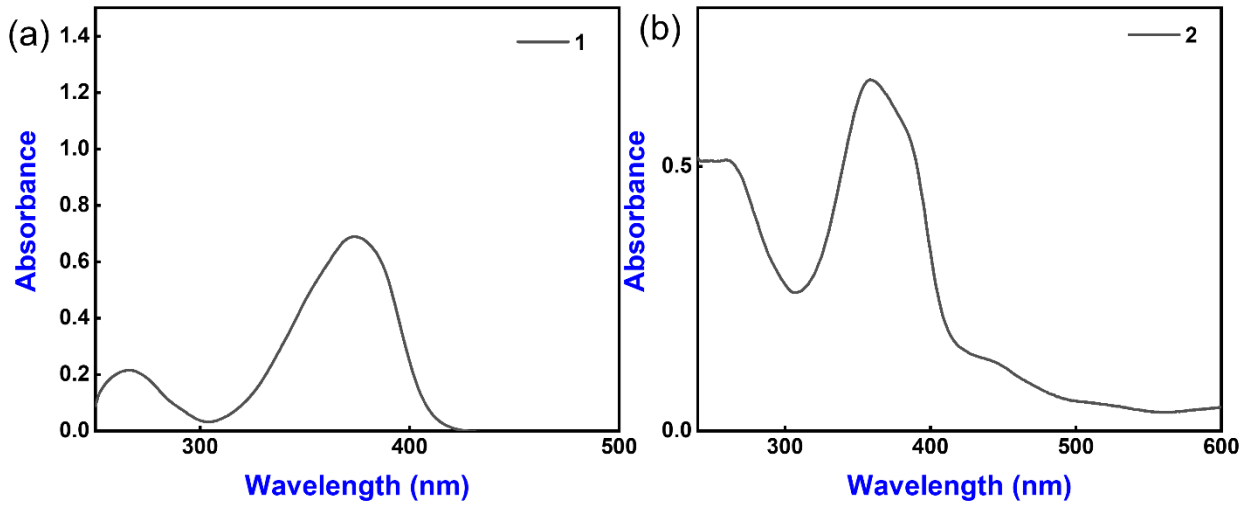

Fig. S7: - UV-Visible spectra of **1** and **2** in EtOH: Water (7:3, v/v, at r.t.).

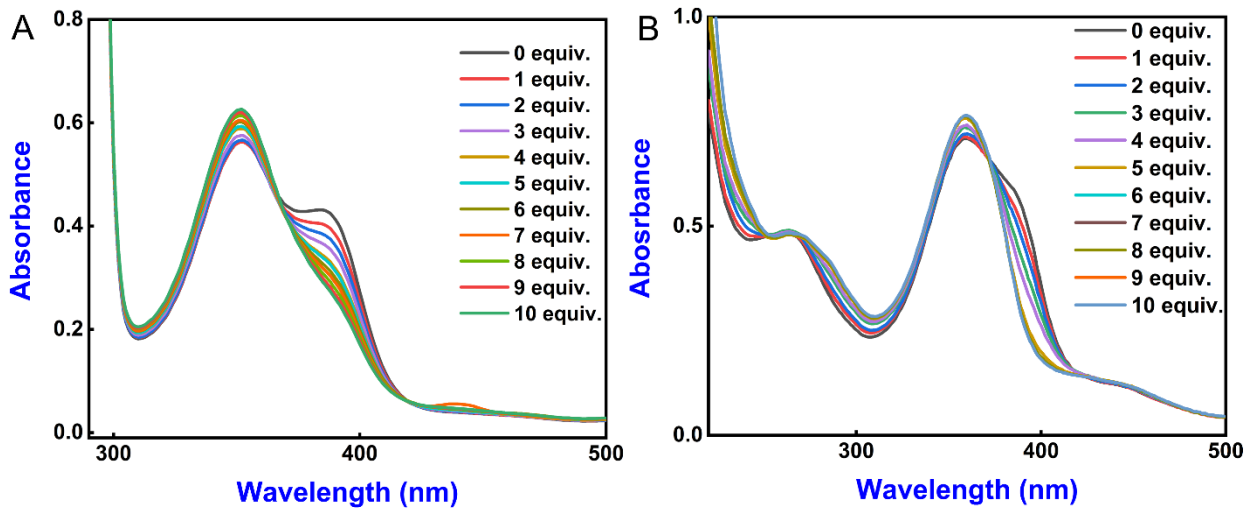

Fig. S8: - UV-Visible titration of the stock solution of **1** and **2** with the conjugative addition of Cu(II) ions (0-10 equiv.) in EtOH:Water (7:3, v/v, at r.t.).

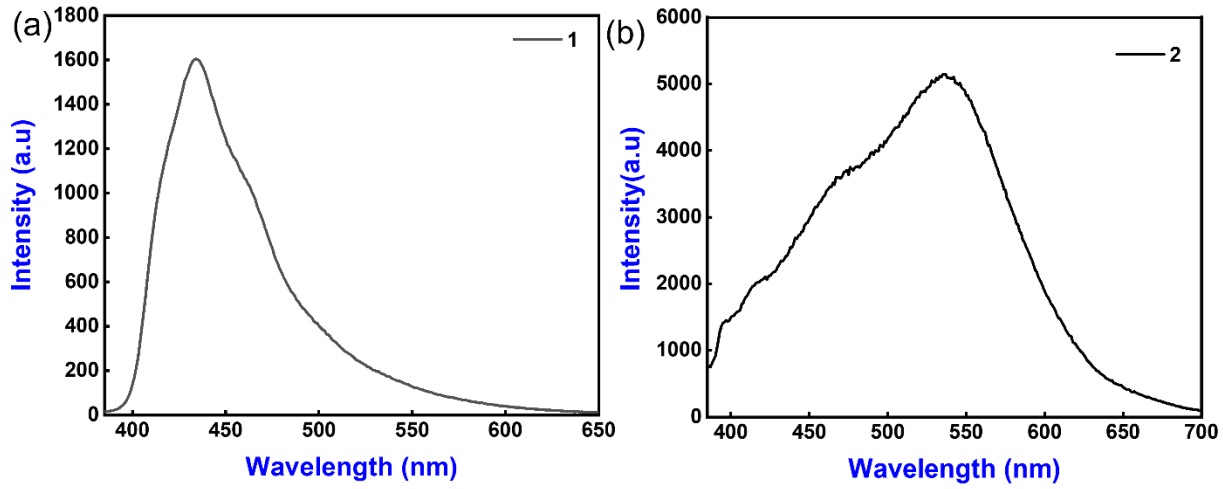

Fig. S9: - Fluorescence spectra of **1** and **2** (10μM) in EtOH: Water (7:3, v/v, at r.t.).

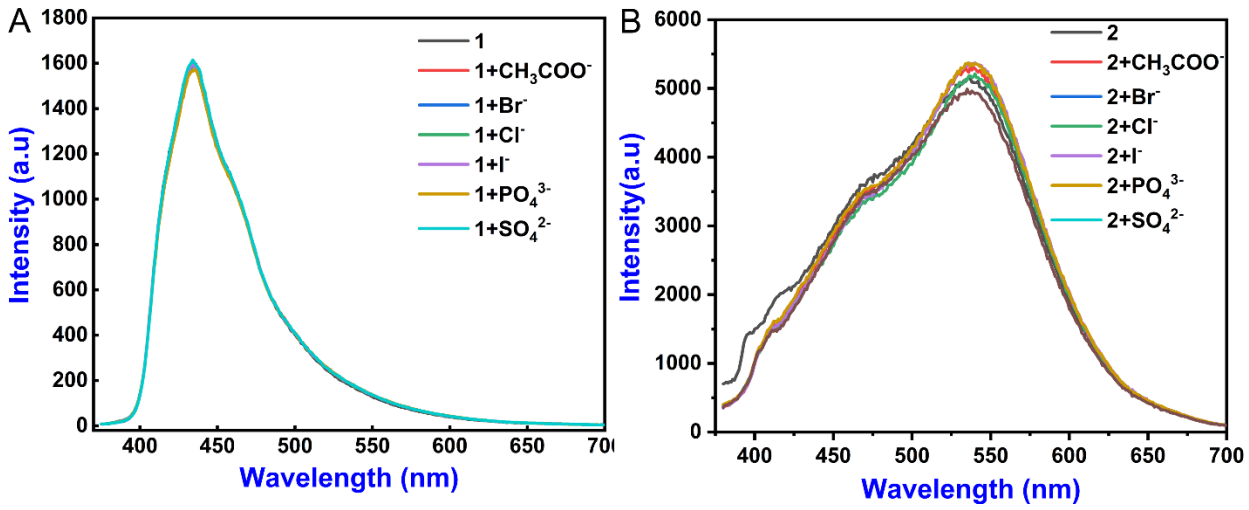

Fig. S10: - Fluorescence sensing of **1** and **2** (10μM) with various anion in EtOH: Water (7:3, v/v, at r.t.).

Determination of the quantum yield.

Standard used: Quinine sulfate salt (QS); QS in 0.54M sulfuric acid has $\phi_f = 0.546$ (at 25˚C)

A 10 μM solution of Quinine sulfate is prepared in 0.5M H_2SO_4, the absorbance maximum of the solution at 345nm, Abs = 0.305. The emission spectrum is also recorded with $\lambda_{exc.}$= 345nm, fluorescence emission is integrated into the range 339-627nm range:1.681×10^8 a.u.

A 10 μM solution of **1** and **1**+Cu(II) is prepared in EtOH: water (7:3, v/v, at r.t.), and the absorbance maximum of the solution at 372 nm shows Abs.= 0.68 for **1** and Abs.= 0.75 for **1**+Zn(II). The emission spectrum is also recorded with $\lambda_{exc.}$= 372 nm for **1** and **1**+Cu(II). Fluorescence emission of **1** was integrated in the range 390-650nm range: 1.135×10^8 a.u. and Fluorescence emission of **1** on the addition of Cu(II) was integrated in the range 390-650 nm range: 6.65×10^7 a.u.

A 10 μM solution of **2** and **2**+Cu(II) is prepared in EtOH: water (7:3, v/v, at r.t.), and the absorbance maximum of the solution at 358 nm shows Abs.= 0.66 for **2** and Abs.= 0.64 for **2**+Cu(II). The emission spectrum is also recorded with $\lambda_{exc.}$= 358 nm for **2** and **2**+Cu(II). Fluorescence emission of **2** was integrated in the range 385-691 nm range: 7.54×10^7 a.u. and Fluorescence emission of **2** on the addition of Cu(II) was integrated in the range 385-691 nm range: 1.69×10^7 a.u.

The formula used for calculating quantum yield

$\Phi_s = \phi_{rf}. I_s/I_{rf}. A_{rf}/A_s. \eta_s/\eta_{rf}$

Where Φ_s is the fluorescence quantum yield of the sample, ϕ_{rf} is the fluorescence quantum yield of the standard reference, I_s and I_{rf} are the integrated emission intensities of the sample and the standard reference respectively, A_{rf} and A_s are the absorbance of the standard reference and the sample at the excitation wavelength, respectively, and n_s and n_{rf} are the refractive indexes of the corresponding solution of sample and reference.

The refractive index of the solvent η_s/η_{rf} were considered one.

Table S1: - Quantum yield of 1 and 2 with and without the addition of Cu(II) ions.

S.No.	Entry	ϕ
1	**1**	0.20
2	**1**+Cu(II)	0.09
3	**2**	0.11
4	**2**+Cu(II)	0.03

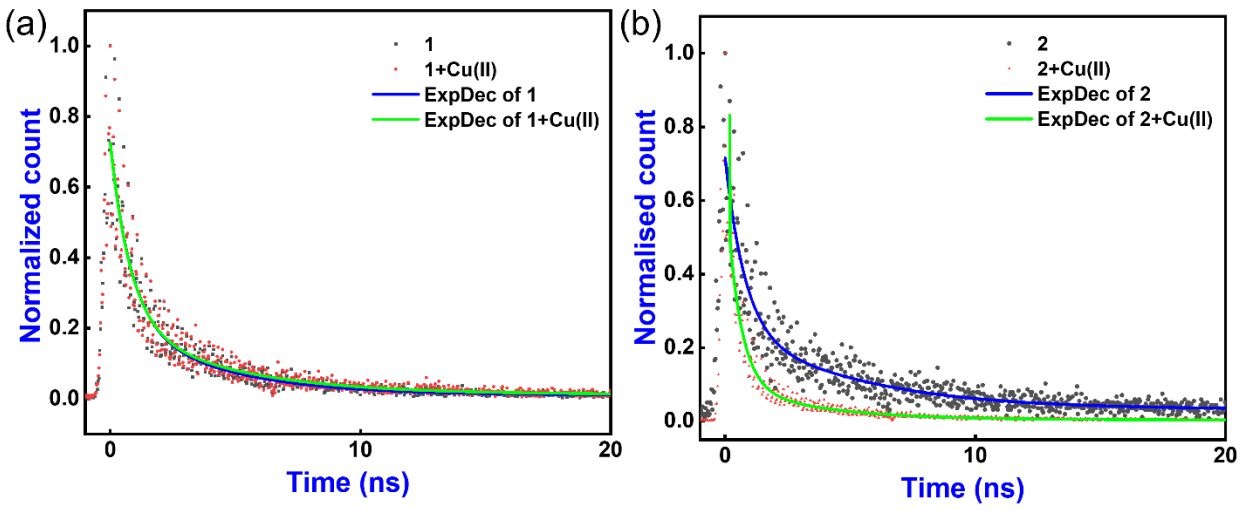

Fig. S11:- Lifetime spectra of stock solution of **1** (a) and **2** (b) (neat) and with the addition of Cu(II) ions in EtOH:Water (7:3, v/v at r.t.) solution

Table S2 Fluorescence decay parameters of pseudopeptidic probes **1** and **2** in ethanol-water solution (7:3, v/v, at rt.).

Entry	(A)	τ (ns)	<τ> (ns)
1	0.33522(A_1)	0.8047(τ_1)	
	0.16739(A_2)	0.80738(τ_2)	1.87
	0.21085(A_3)	4.40839(τ_3)	
1+Cu(II)	0.80617(A_1)	0.80617(τ_1)	
	0.13556(A_2)	0.80637(τ_2)	1.78
	0.22592(A_3)	3.89881(τ_3)	

2	4.79091(A_1)	0.00429(τ_1)	
	0.55736(A_2)	0.54423(τ_2)	1.32
	0.1002(A_3)	3.41099(τ_3)	
2+Cu(II)	2.23637(A_1)	1.00096(τ_1)	
	1.8233(A_2)	109087(τ_2)	1.26
	0.26991(A_3)	4.51356(τ_3)	

Dynamic parameters determined from $A_1\exp(-x/\tau_1) + A_2\exp(-x/\tau_2) + A_3\exp(-x/\tau_2) + y_0$

The weighted mean lifetime $\langle\tau\rangle$ was calculated by using following equation:

$$\langle\tau\rangle = (A_1\tau_1 + A_2\tau_2 + A_3\tau_3) / (A_1 + A_2 + A_3)$$

where, $A_1/A_2/A_3$ and $\tau_1/\tau_2/\tau_3$ are the fractions (A) and lifetimes (τ) respectively.

Solution concentration = 10 μM.

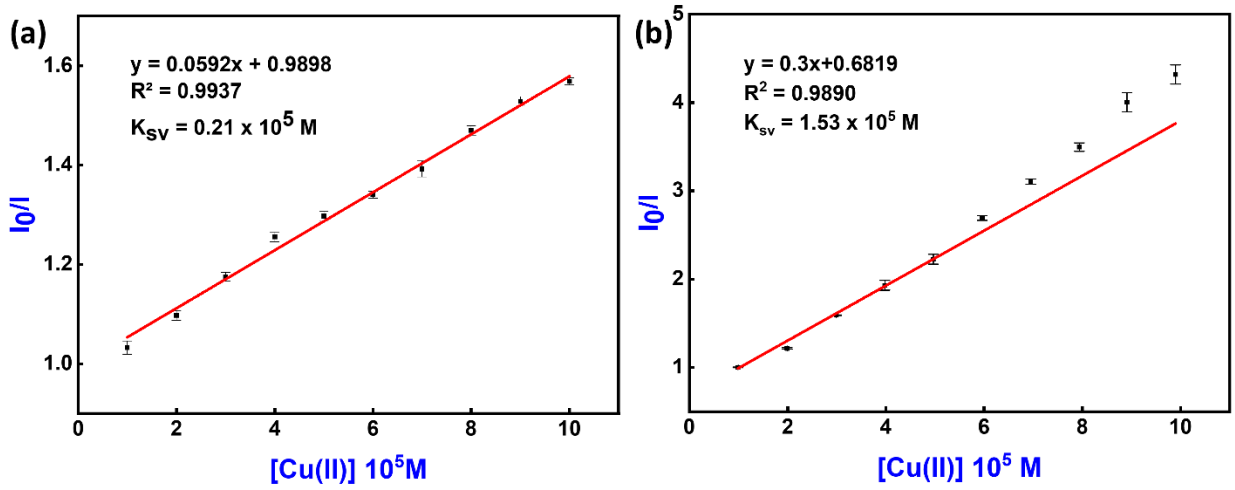

Fig. S12 - Stern-Volmer plot of **1** (a) and **2** (b) with respect to the concentration of Cu(II) ions in EtOH:Water (7:3, v/v, at r.t.).

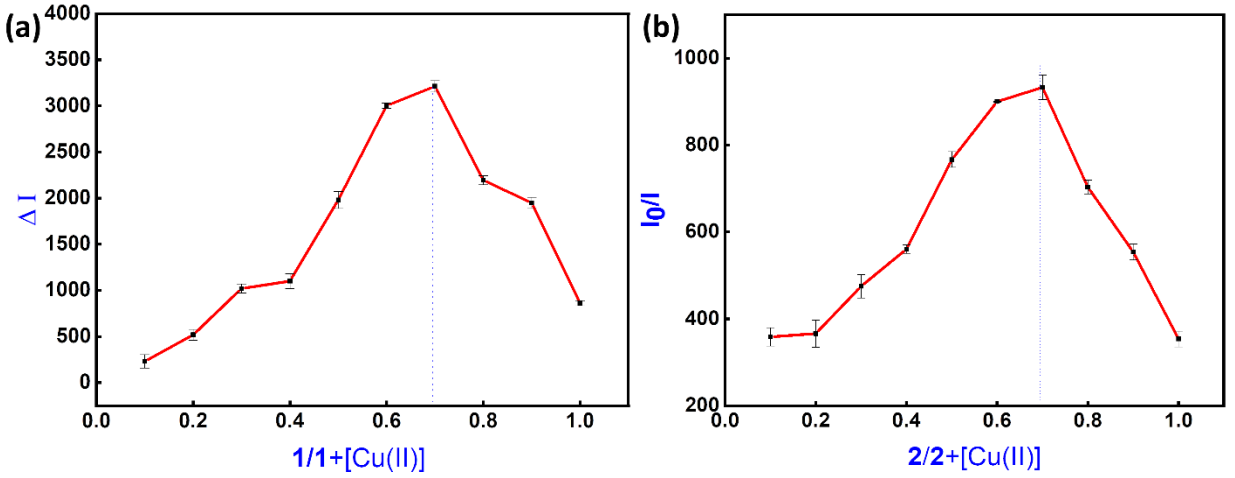

Fig. S13: - Jobs plot of aqueous stock solution of **1** (a) and **2** (b) toward varying concentrations of Cu(II) ions in ETOH:Water (7:3, v/v, at r.t.)

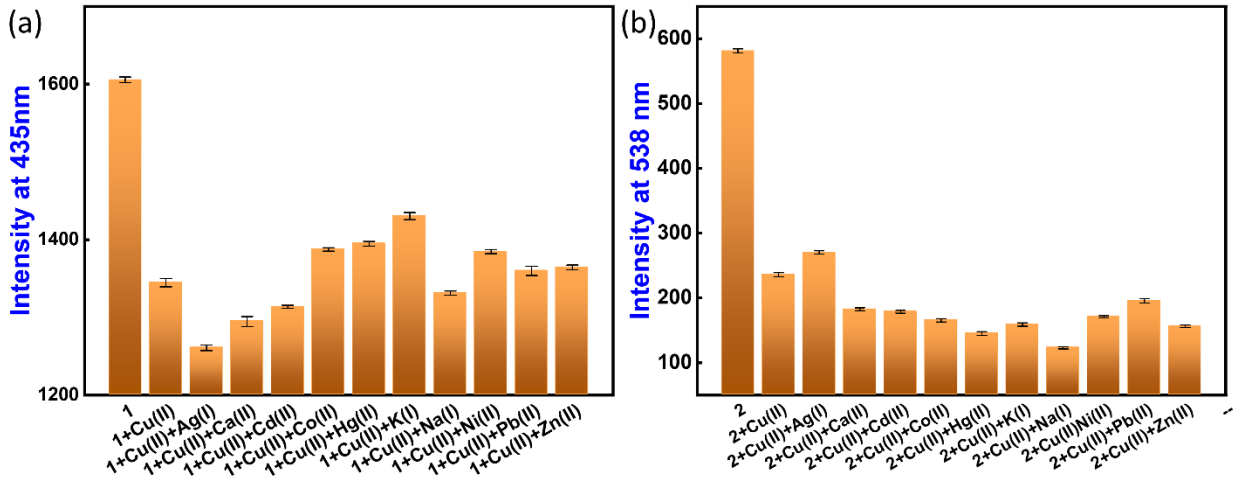

Fig. S14:- Interference experiments of aqueous stock solution of **1** (a) and **2** (b) toward Cu(II) ions and other metal ions in EtOH:Water (7:3, v/v, at r.t.)

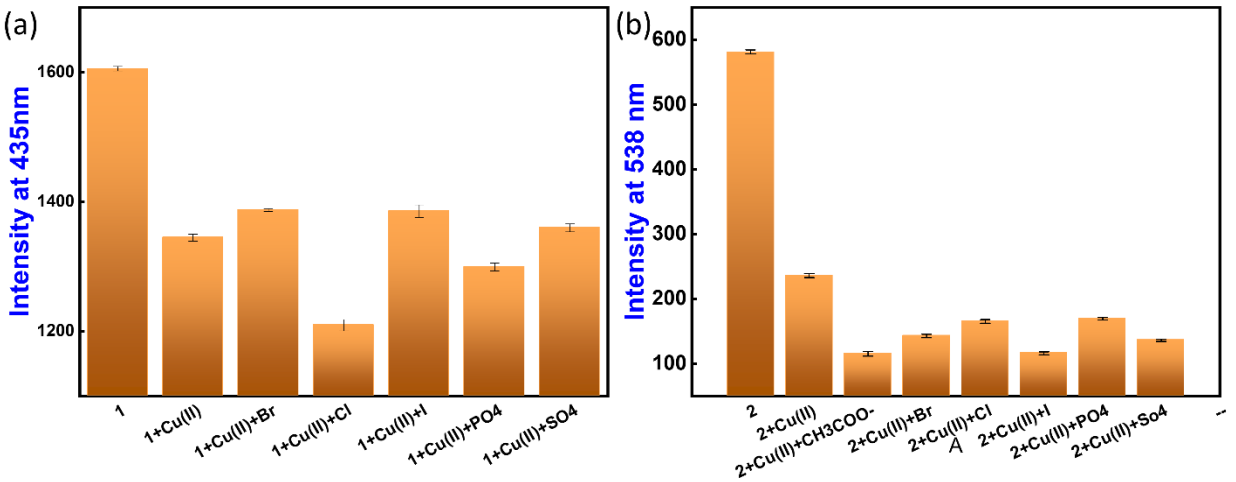

Fig. S15: - Interference experiments of aqueous stock solution of **1** (a) and **2** (b) toward Cu(II) ions and other anions in EtOH:Water (7:3, v/v, at r.t.).

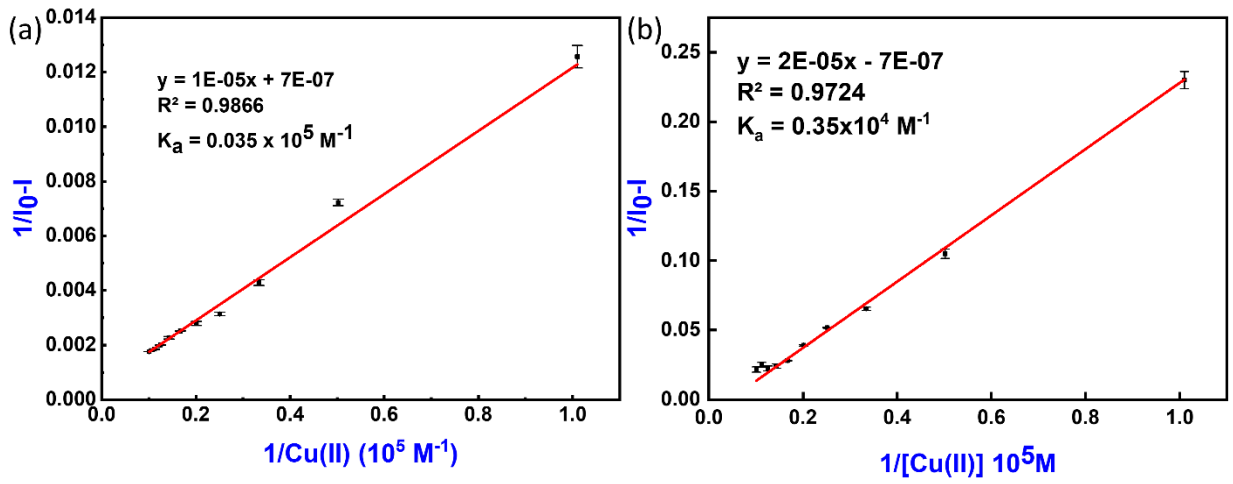

Fig. S16: - Benesi-Hildebrand plot of **1** (a) and **2** (B) with the varying concentration of Cu(II) ions in EtOH: Water (7:3, v/v, rt.)

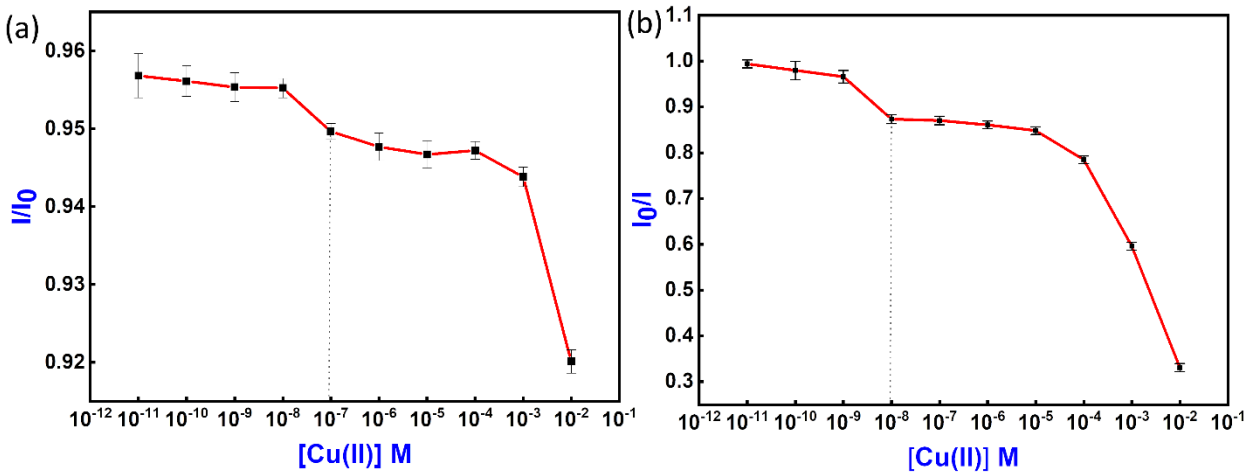

Fig. S17: - Fluorescence sensitivity of **1** (a) and **2** (b) in the presence of a different concentration of Cu(II) (10^{-11} to 10^{-3} M) ions in EtOH:Water (7:3, v/v, at r.t.)

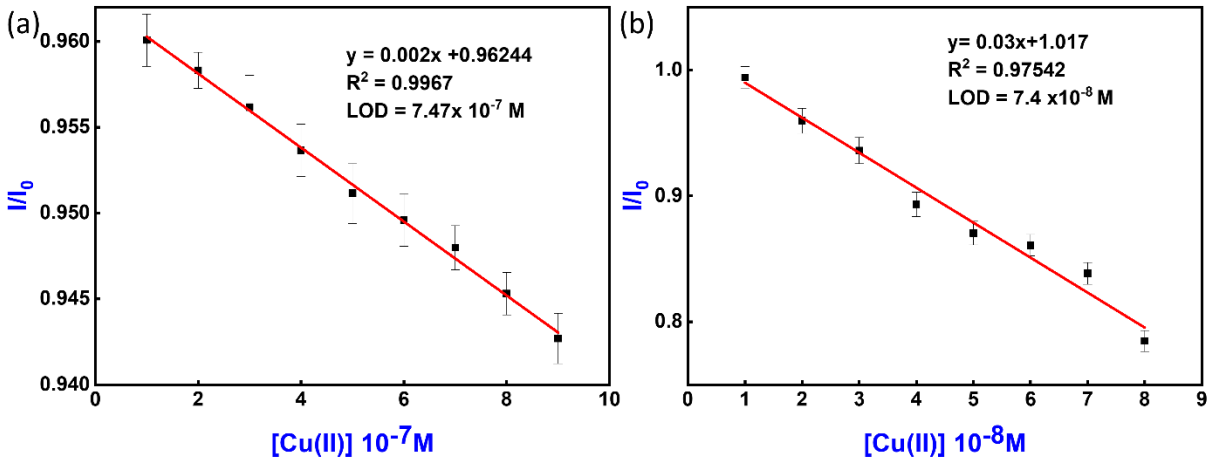

Fig. S18: - (a) Fluorescence sensitivity of **1** in the presence of a different concentration of Cu(II) (1 x 10^{-7} to 9 x 10^{-7} M) ions in EtOH:Water (7:3, v/v, at r.t.). (b) Fluorescence sensitivity of **2** in the presence of a different concentration of Cu(II) (1 x 10^{-8} to 9 x 10^{-8} M) ions in EtOH:Water (7:3, v/v, at r.t.).

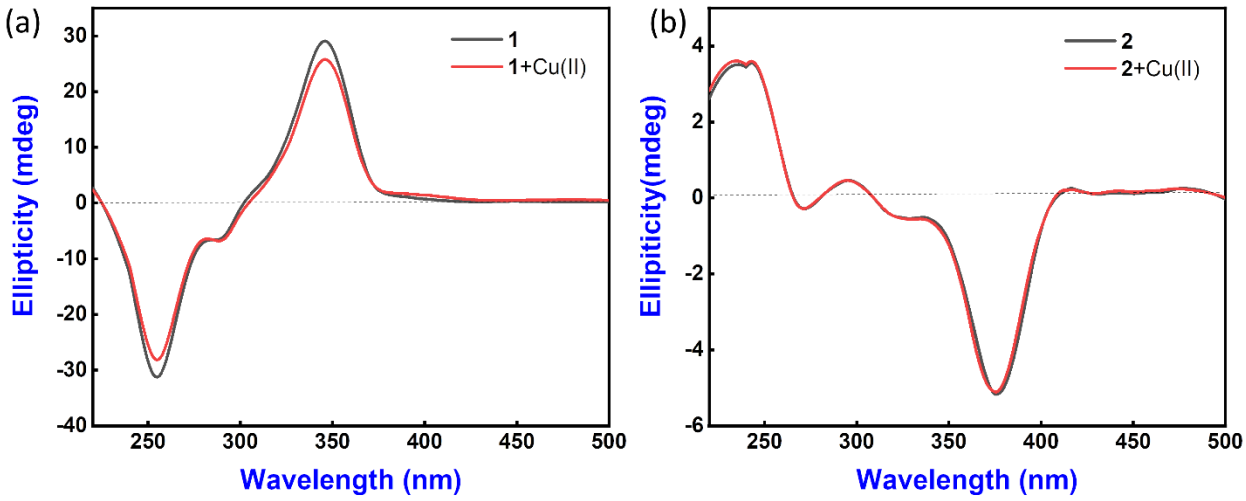

Fig. S19: - CD spectra of stock solution of chemosensor **1** (A) and **2** (B) (neat) and with the addition of Cu(II) ions in Ethanol: Water (7:3, v/v, at r.t.) solution.

Table S3: - Comparison with previously reported fluorescence-based sensors for Cu(II) ions.

S. No.	Probe	Analyte detect	Solvent system	Fluorescence effect	Binding constant	LOD (μM)	Ref.
1	**1** **2**	Cu(II)	EtOH:Water (7:3, v/v)	Quenching	0.035×10^5 M^{-1} 0.02×10^5 M^{-1}	0.831 0.074	**This work**
2	**3**	Cu(II)	Tris-HCl (CH_3CN/H_2O, v/v, 3:2, pH 7.24)	Quenching	2.2×10^6	0.46	1
3	**6**	Cu(II)	PBS (pH 7.4)	Quenching	1.879×10^5	0.0833	2
4	**7**	Cu(II)	CH_3CN/H_2O (v/v, 7:3)	Quenching	3×10^{10} $molL^{-2}$	0.503	3
5	**8**	Cu(II)	THF:H_2O (v/v, 1:9)	Quenching	4×10^9 M^{-2}	1.5	4
6	**10**	Cu(II)	CH_3OH/H_2O (v/v, 1:1)	Quenching	1.88×10^{-4}	5.36	5
7	**11**	Cu(II)	CH_3CN	Quenching	-	0.19	6
8	**12** **13** **14** **15**	Cu(II)	DMSO/H_2O (v/v, 2:8) HEPES buffer (pH 7.4)	Quenching	31.22×10^4 31.36×10^4 33.51×10^4 33.57×10^4	0.301 0.482 0.517 0.623	7
9	**16**	Cu(II)	CH_3CN	Enhancement	1.96×10^6	0.972	8

10	**17**	Cu(II)	CH_3OH:Water (8:2, v/v)	Enhancement	4.0×10^4	0.170	9
11	**18**	Cu(II)	Aqueous solution	Enhancement	5.38×10^4	0.592	10
12	**19**	Cu(II)	CH_3CN	Enhancement	9.877×10^4	2.5	11
13	**20**	Cu(II)	PBS (pH =7.4)	Enhancement	-	23.60	12
14	**21**	Cu(II)	CH_3CN: H_2O (7:3, v/v)	Enhancement	3.12×10^4	2.11	13
15	**22** **23** **24** **25**	Cu(II)	CH_3CN/DMSO (v/v, 99:1)	Enhancement	3.12×10^4 3.12×10^4 3.12×10^4 3.12×10^4	7.6 5.8 4.3 2.8	14

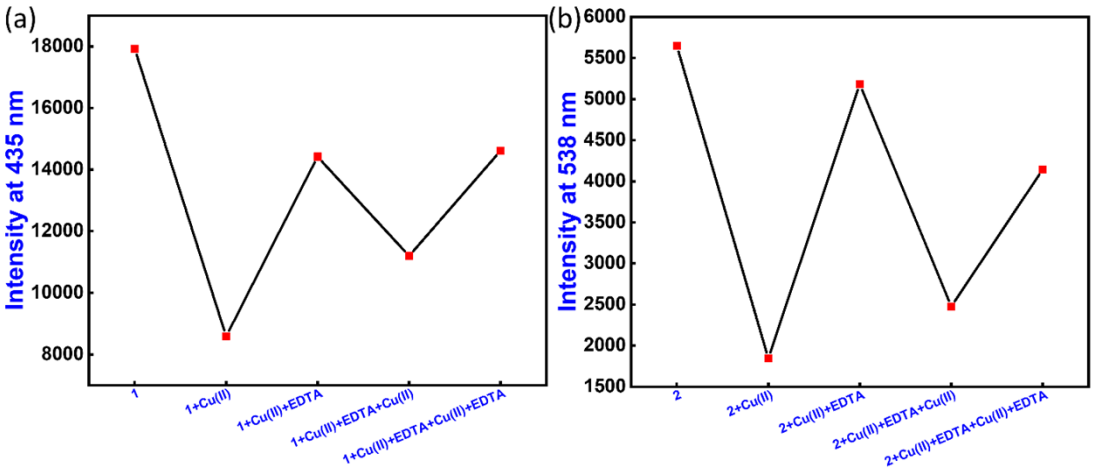

Fig. S20: - Reversibility plot of 1 and 2 with respect to the addition of Cu(II) ion and EDTA solution.

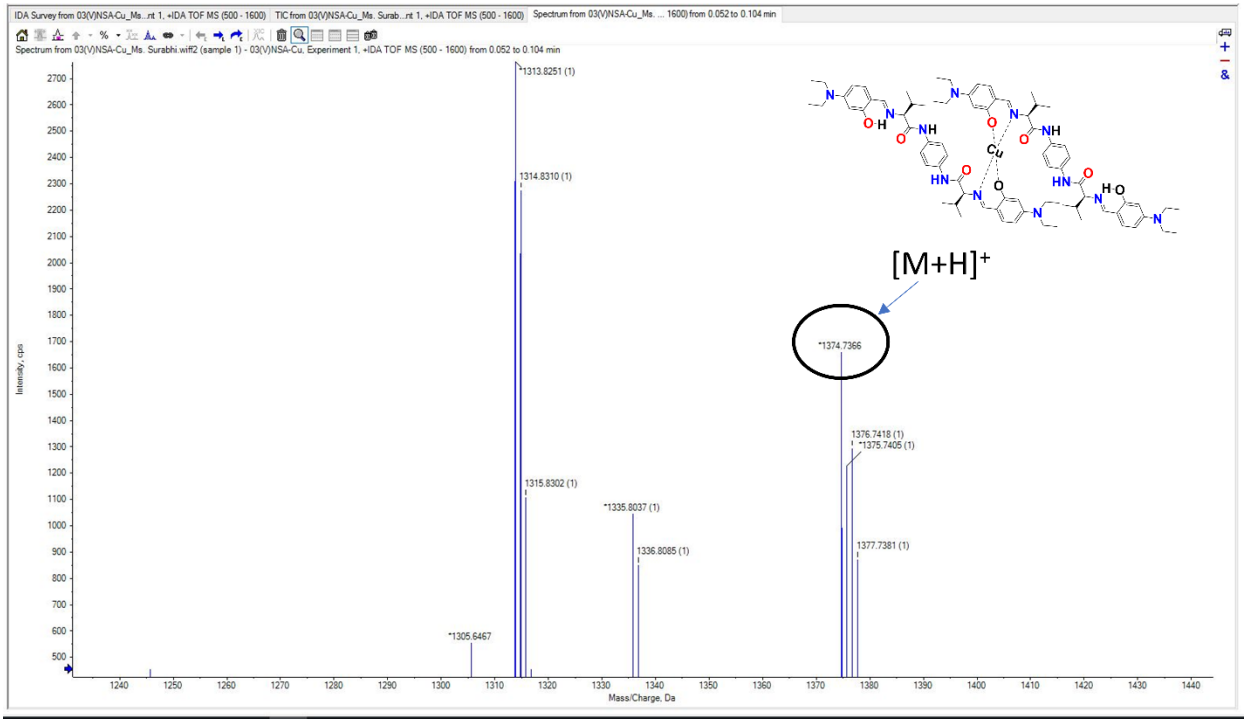

Fig. S21: - HRMS (ESI-TOF) spectra of **1**+Cu(II).

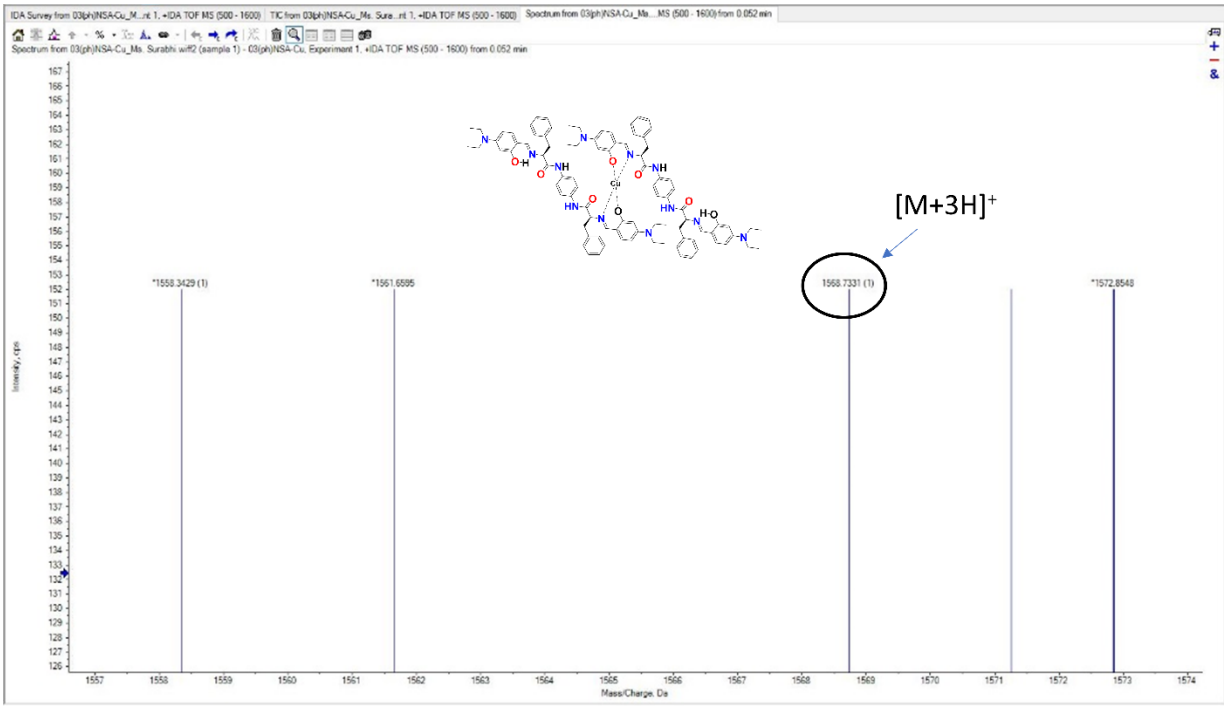

Fig. S22: -HRMS (ESI-TOF) spectra of **2**+Cu(II).

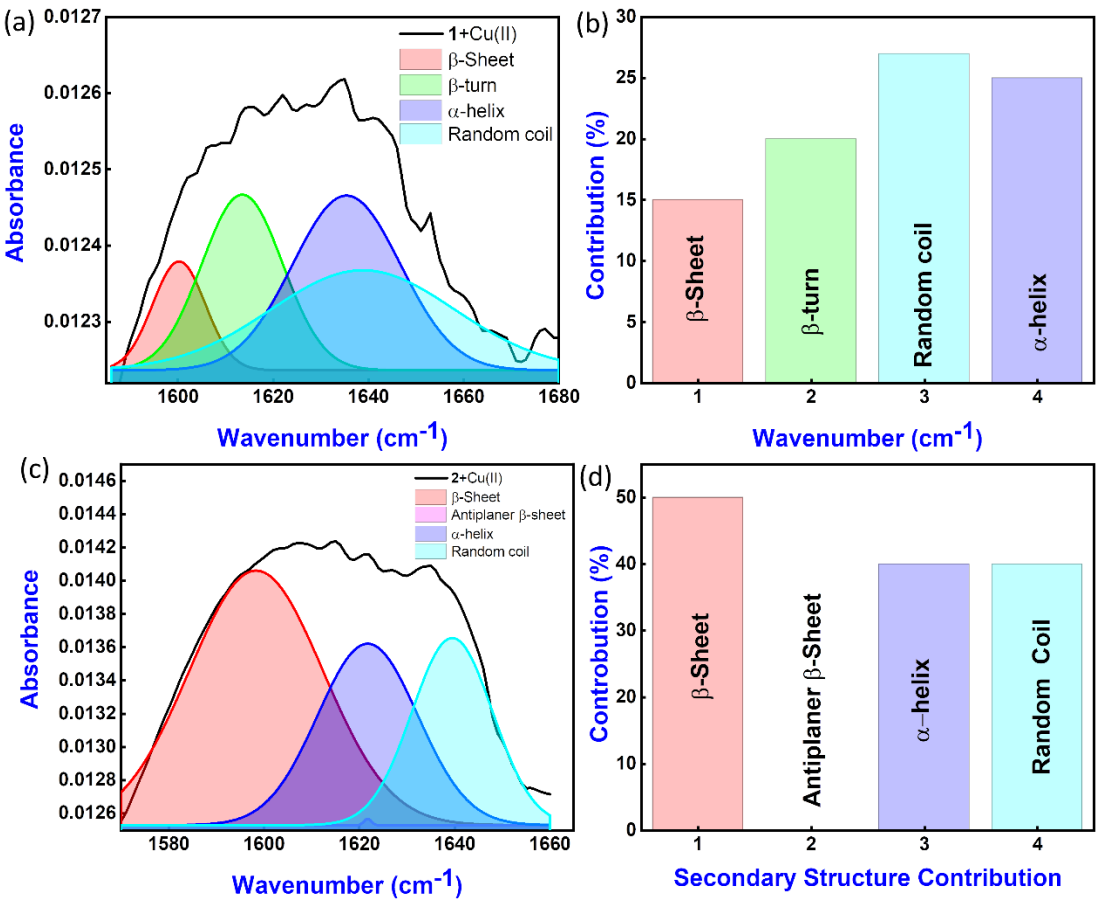

Fig. S23: - (a) The FT-IR spectrum of **1**+Cu(II) with the representation of its deconvolution (shades) to provide a contribution of secondary structures, (b) the percentage contribution of corresponding secondary structure in amide region through self-assembly. (c) The FT-IR spectrum of **2**+Cu(II) with the representation of its deconvolution (shades). (d) percentage contribution of corresponding secondary structure in amide region through self-assembly. Deconvolution was done by fitting multiple Gaussian peaks in the amide region ranging from 1570 to 1680 cm^{-1}.

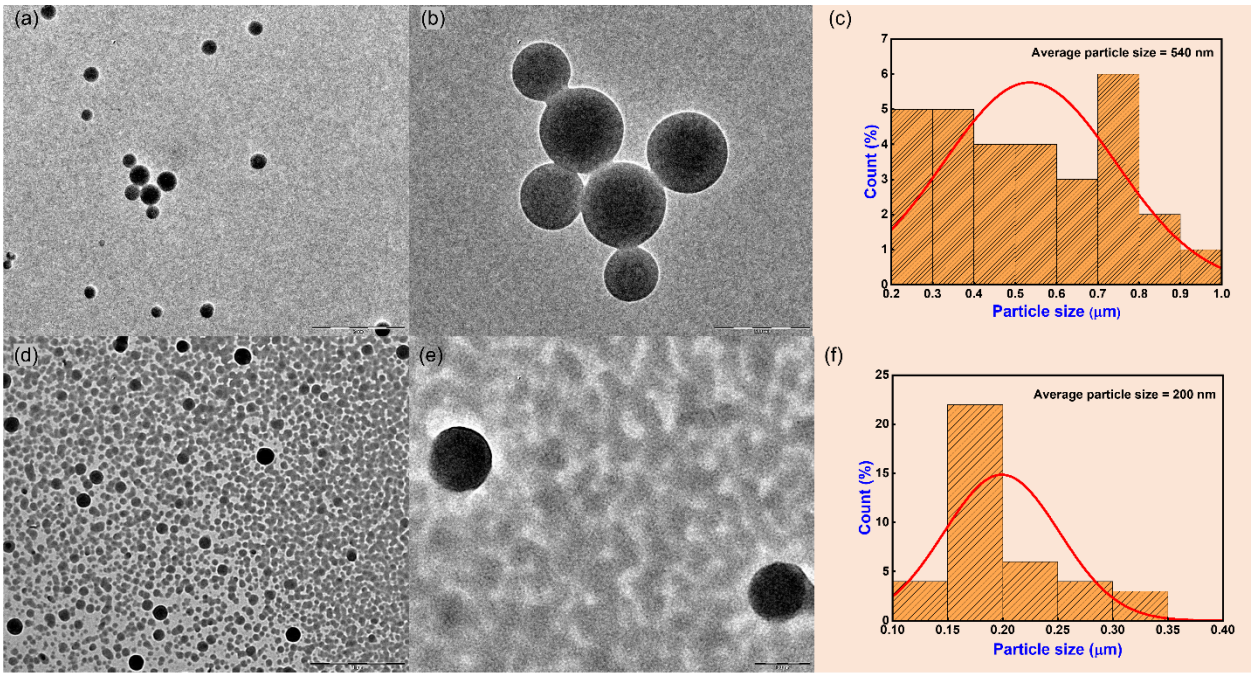

Fig. S24: - Electron microscopy images of self-assembly neat **1** (a) 2D representation. (b) zoomed image of the 2D representation of **1**. (c) Average particle size distribution of **1**. (d) 2D representation of self-assembly of **1**+Cu(II). (e) Zoomed image of the 2D representation of **1**+Cu(II). (f) Average particle size distribution of **1**+Cu(II).

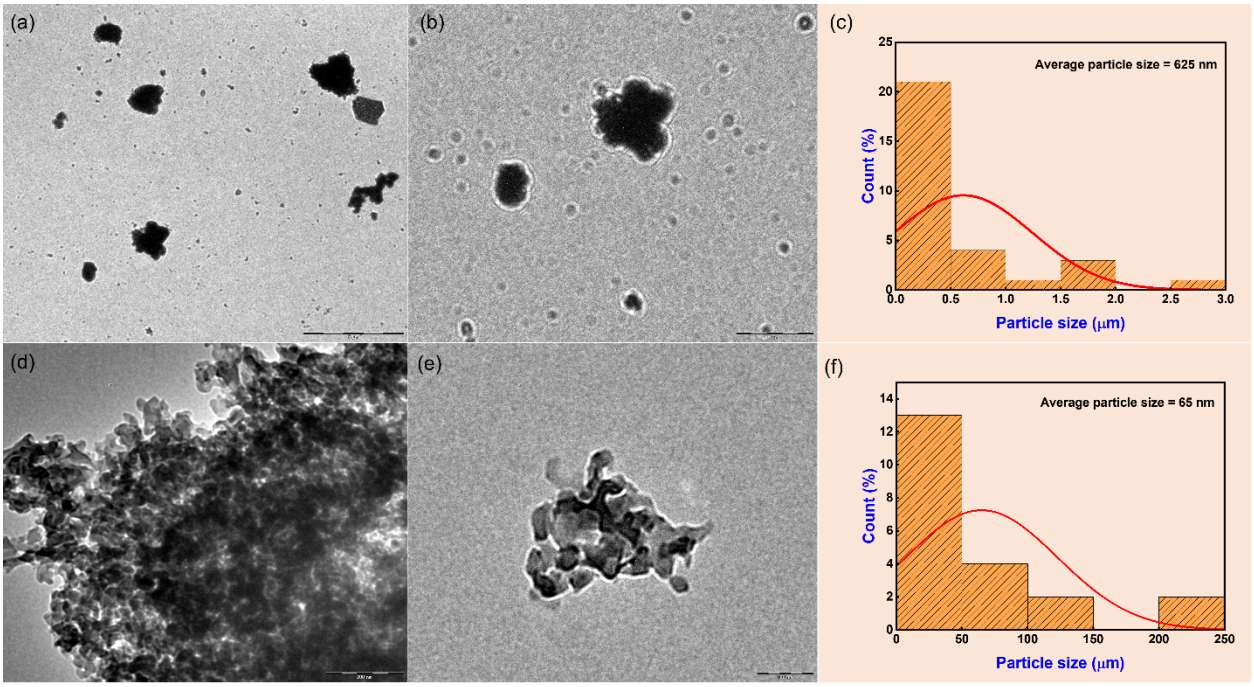

Fig. S25: - Electron microscopy images of self-assembly neat **2**, (a) 2D representation. (b) zoomed image of the 2D representation of **2**. (c) Average particle size distribution of **2**. (d) 2D representation of **2**+Cu(II). (e) Zoomed image of 2D representation of **2**+Cu(II). (f) Average particle size distribution of **2**+Cu(II).

Table S4: - Quantitative determination of spiked quantity of Cu(II) ions in the various water sample

S. No.	Sample	Entry	Zn(II) added (μM)	Zn(II) found (μM)	% Recovery	%RSD (n=3)
1	Lake Water	**1** **2**	6, 10 6, 10	7.4, 11.1 5.92, 9.8	123, 111	4.55, 10.38 0.029, 0.048
2	River Water	**1** **2**	6, 10 6, 10	7.1, 10.8 6.14, 10.03	118, 108	3.27, 5.05 0.079, 0.63
3	Pond Water	**1** **2**	6, 10 6, 10	6.6, 10.7 6.42, 10.76	110, 107	2.51, 6.74 0.35, 0.43
4	Tap Water	**1** **2**	6, 10 6, 10	6.1, 10.4 6.3, 10.2	101, 104	3.66, 4.36 0.093, 4.35

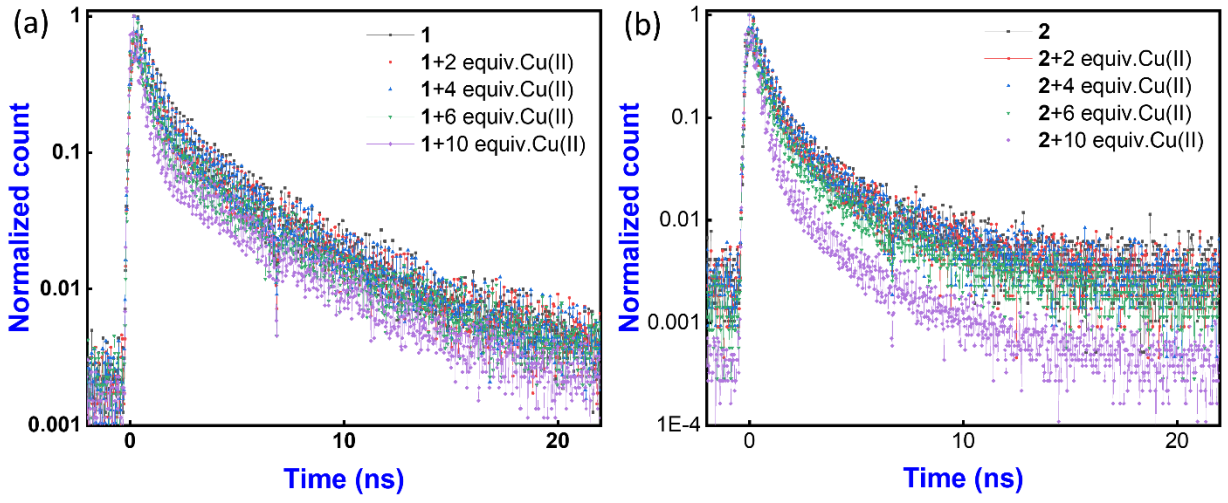

Fig. S26: - Lifetime spectra of stock solution of **1** (a) and **2** (b) (neat) and with the addition of various concentrations of Cu(II) ions (0-10equiv.) in EtOH:Water (7:3, v/v at r.t.) solution.

Table S5: - Fluorescence decay parameters of pseudopeptidic probes **1** and **2** on addition of various concentrations of Cu(II) ions (0-10equiv.) in ethanol-water solution (7:3, v/v, at rt.).

Entry	(A_1)	(A_2)	(A_3)	τ_1 (ns)	τ_2 (ns)	τ_3 (ns)	$<\tau>$ (ns)
1	0.3352	0.1673	0.21085	0.8047	0.80738	4.40839	1.87
1+Cu(II) (10 μL)	0.3014	0.3986	0.2949	0.7339	0.7460	4.4787	1.85
1+Cu(II) (20 μL)	0.4032	0.2949	0.3556	0.6788	0.6787	4.0639	1.82
1+Cu(II) (30 μL)	0.4216	0.30036	0.3553	0.6901	0.6899	4.0129	1.78
1+Cu(II) (30 μL)	0.5304	0.6226	0.3397	0.5221	0.5993	3.9831	1.44
2	4.79091	0.55736	0.1002	0.00429	0.54423	3.41099	1.32
2+Cu(II)	0.4205	0.3871	0.1417	0.7586	0.7760	4.4687	1.31
2+Cu(II)	0.4033	0.4039	0.1568	0.7296	0.7297	4.2449	1.30
2+Cu(II)	0.5511	0.3179	0.1538	0.5915	0.7915	4.1041	1.21
2+Cu(II)	0.5834	0.3757	0.1932	0.4670	0.7197	4.2114	1.17

Dynamic parameters determined from $A_1\exp(-x/\tau_1) + A_2\exp(-x/\tau_2) + A_3\exp(-x/\tau_2) + y_0$

The weighted mean lifetime $<\tau>$ was calculated by using following equation:

$$<\tau> = (A_1\tau_1 + A_2\tau_2 + A_3\tau_3) / (A_1 + A_2 + A_3)$$

where, $A_1/A_2/A_3$ and $\tau_1/\tau_2/\tau_3$ are the fractions (A) and lifetimes (τ) respectively.

Solution concentration = 10 μM.

References: -

1. Y. Zhang, X. Guo, X. Tian, A. Liu, L. Jia, *Sens. Actuators B Chem.*, **2015**, 218, 37-41.
2. M. Li, S. Sheth, Y. Xu and Q. Song, *Microchem. J.*, **2020,** 156, 104848.
3. L. G. T. A. Duarte, F. L. Coelho, J. C. Germino, G. G. da Costa, J. F. Berbigier, F. S. Rodembusch, T. D. Z. Atvars, *Dyes Pigm.*, **2020,** 181, 108566.
4. D. Li, J. Li, Y. Duan, B. Zhao, B. Ji, *Anal. Methods*, **2016,** 8, 6013-6016.
5. Y. Chen, L. Zhao, J. Jiang, *Spectrochim. Acta-A Mol. Biomol. Spectrosc.*, **2017,** 175, 269-275.
6. S.-J. He, Y.-W. Xie, Q.-Y. Chen, *Spectrochim. Acta-A Mol. Biomol. Spectrosc.*, **2018**, 195, 210-214.
7. K. Mal, B. Naskar, T. Chaudhuri, C. Prodhan, S. Goswami, K. Chaudhuri and C. Mukhopadhyay, *J. Photochem. Photobio. A Chem.*, 2020, **389**, 112211.
8. M. Shellaiah, Y. H. Wu, A. Singh, M. V. RamakrishnamRaju, H. C. Lin, *J. Mater. Chem. A*, 2013, **1,** 1310-1318.
9. C. Zhang, B. Gao, Q. Zhang, G. Zhang, S. Shuang, C. Dong, *Talanta,* 2016, **154,** 278-283.

10. G. Li, L. Bai, F.Tao, A. Deng, L. Wang, *Analyst*, 2018, **143**, 5395-5403.

11. N. Chakraborty, A. Chakraborty, S. Das, *J. Luminescence,* 2018, **199**, 302-309.

12. V. Kshtriya, B. Koshti, D. K. Pandey, S. Kharbanda, C. K. P, D. K. Singh, D. Bhatia, N. Gour, Soft Matter, 2021, **17**, 4304-4316.

13. F. Abebe, P. Perkins, R. Shaw, S. Tadesse, *J Mol Struct.* 2020, **1205**, 127594.

14. A. Ramdass, V. Sathish, M. Velayudham, P. Thanasekaran, S. Umapathy, S. Rajagopal, RSC Adv. 2015, **5**, 38479-38488.